REPORT DOCUMENTATION PAGE

Form Approved
OMB No. 0704-0188

1. AGENCY USE ONLY *(Leave blank)*	2. REPORT DATE	3. REPORT TYPE AND DATES COVERED
	May 1996	FINAL

4. TITLE AND SUBTITLE

Ventilation-Perfusion Alterations after Inhalation Injury in an Ovine Model

5. FUNDING NUMBERS

3A16110A91C

6. AUTHOR(S)

Takeshi Shimazu, Tetsuo Yukioka, Hisashi Ikeuchi, Arthur D. Mason, Jr., Peter D. Wagner, and Basil A. Pruitt, Jr.

7. PERFORMING ORGANIZATION NAME(S) AND ADDRESS(ES)

US Army Institute of Surgical Research Fort Sam Houston, Texas 78234

8. PERFORMING ORGANIZATION REPORT NUMBER

9. SPONSORING / MONITORING AGENCY NAME(S) AND ADDRESS(ES)

US Army Medical Research and Materiel Command
Fort Detrick
Frederick, MD 21702

10. SPONSORING / MONITORING AGENCY REPORT NUMBER

11. SUPPLEMENTARY NOTES

Published In: Journal of Applied Physiology 81(5): 2250-2259, 1996

12a. DISTRIBUTION / AVAILABILITY STATEMENT

APPROVED FOR PUBLIC RELEASE
DISTRIBUTION UNLIMITED

12b. DISTRIBUTION CODE

A

13. ABSTRACT *(Maximum 200 words)*

Ventilation-perfusion alterations after smoke inhalation injury in an ovine model. *J. Appl. Physiol.* 81(5): 2250–2259, 1996.—To study the pathophysiological mechanism of progressive hypoxemia after smoke inhalation injury, alterations in ventilation-perfusion ratio ($\dot{V}A/\dot{Q}$) were studied in an ovine model by using the multiple inert gas elimination technique. Because ethane was detected in expired gas of some sheep, we replaced ethane with krypton, which was a unique application of the multiple inert gas elimination technique when one of the experimental gases is present in the inspirate. Severity-related changes were studied 24 h after injury in control and mild, moderate, and severe inhalation injury groups. Time-related changes were studied in controls and sheep with moderate injury at 6, 12, 24, and 72 h. Arterial Po_2 decreased progressively with severity of injury as well as with time. In smoke-exposed animals, blood flow was recruited to low $\dot{V}A/\dot{Q}$ compartment ($0 < \dot{V}A/\dot{Q} < 0.1$; $17.6 \pm 10.6\%$ of cardiac output, 24 h, moderate injury) from normal $\dot{V}A/\dot{Q}$ compartment ($0.1 < \dot{V}A/\dot{Q} < 10$). However, increases in true shunt ($\dot{V}A/\dot{Q} = 0$; $5.6 \pm 2.5\%$, 24 h, moderate injury) and dead space were not consistent findings. The $\dot{V}A/\dot{Q}$ patterns suggest the primary change in smoke inhalation injury to be a disturbance of ventilation.

lung injury; severity-related changes; time-related changes; low ventilation-perfusion; krypton; gas chromatography-mass spectrometry

14. SUBJECT TERMS	15. NUMBER OF PAGES
lung injury; severity-related changes; time-related changes; low ventilation perfusion; krypton; gas chromatography-mass spectrometry	10
	16. PRICE CODE

17. SECURITY CLASSIFICATION OF REPORT	18. SECURITY CLASSIFICATION OF THIS PAGE	19. SECURITY CLASSIFICATION OF ABSTRACT	20. LIMITATION OF ABSTRACT
UNCLASSIFIED	UNCLASSIFIED	UNCLASSIFIED	

Ventilation-perfusion alterations after smoke inhalation injury in an ovine model

TAKESHI SHIMAZU, TETSUO YUKIOKA, HISASHI IKEUCHI,
ARTHUR D. MASON, JR., PETER D. WAGNER, AND BASIL A. PRUITT, JR.
United States Army Institute of Surgical Research, Fort Sam Houston, Texas 78234-5012; Department of Traumatology, Osaka University Medical School, Osaka 565; Department of Traumatology and Critical Care Medicine, Kyorin University School of Medicine, Tokyo 181, Japan; and Department of Medicine, University of California, San Diego, La Jolla, California 92093-0623

Shimazu, Takeshi, Tetsuo Yukioka, Hisashi Ikeuchi, Arthur D. Mason, Jr., Peter D. Wagner, and Basil A. Pruitt, Jr. Ventilation-perfusion alterations after smoke inhalation injury in an ovine model. *J. Appl. Physiol.* 81(5): 2250–2259, 1996.—To study the pathophysiological mechanism of progressive hypoxemia after smoke inhalation injury, alterations in ventilation-perfusion ratio ($\dot{V}_A/\dot{Q}$) were studied in an ovine model by using the multiple inert gas elimination technique. Because ethane was detected in expired gas of some sheep, we replaced ethane with krypton, which was a unique application of the multiple inert gas elimination technique when one of the experimental gases is present in the inspirate. Severity-related changes were studied 24 h after injury in control and mild, moderate, and severe inhalation injury groups. Time-related changes were studied in controls and sheep with moderate injury at 6, 12, 24, and 72 h. Arterial P_{O_2} decreased progressively with severity of injury as well as with time. In smoke-exposed animals, blood flow was recruited to low $\dot{V}_A/\dot{Q}$ compartment ($0 < \dot{V}_A/\dot{Q} < 0.1$; 17.6 ± 10.6% of cardiac output, 24 h, moderate injury) from normal $\dot{V}_A/\dot{Q}$ compartment ($0.1 < \dot{V}_A/\dot{Q} < 10$). However, increases in true shunt ($\dot{V}_A/\dot{Q} = 0$; 5.6 ± 2.5%, 24 h, moderate injury) and dead space were not consistent findings. The $\dot{V}_A/\dot{Q}$ patterns suggest the primary change in smoke inhalation injury to be a disturbance of ventilation.

lung injury; severity-related changes; time-related changes; low ventilation-perfusion; krypton; gas chromatography-mass spectrometry

SMOKE INHALATION INJURY is one of the primary determinants of survival after major burns. Smoke inhalation injury by itself increases mortality of burn patients up to a maximum of 20% (21). Such injury has commanded wide clinical interest, but its pathophysiological mechanisms are not clearly defined (11).

To elucidate the mechanism of progressive hypoxemia after smoke inhalation injury, we have used the multiple inert gas elimination technique (MIGET) in an ovine model, which is reproducible and dose responsive (20). The MIGET, using gas chromatography (GC), was developed by Wagner et al. (26, 28) in 1974 to determine continuous distribution of ventilation-perfusion ratios ($\dot{V}_A/\dot{Q}$). By use of this method, the true shunt ($\dot{V}_A/\dot{Q} = 0$) and the low $\dot{V}_A/\dot{Q}$ ($0 < \dot{V}_A/\dot{Q} < 0.1$) can be differentiated, enabling detailed analysis of the mechanism of respiratory impairment. The technique has been applied extensively in evaluation of respiratory pathophysiology (5, 10, 18, 24, 27). For smoke inhalation injury, however, there has been only one report of the use of MIGET in a small number of patients and animals (16). To perform MIGET by using sheep, we substituted krypton for ethane as one of the six gases because ethane as well as methane was detected in the expired gas. With krypton being present in trace amounts in the inspirate (~1.1 parts/million in the atmosphere), this is a unique application of the MIGET. In the present study, we have characterized $\dot{V}_A/\dot{Q}$ changes after smoke inhalation injury in terms of severity-related and time-related alterations to obtain physiological information for use in respiratory management.

MATERIALS AND METHODS

Study design and animals. Forty-seven neutered male sheep weighing 22–50 kg (33.2 ± 5.6 kg) were used in this study. Severity-related changes were studied in 21 sheep consisting of 5 uninjured controls and 16 exposed individually to amounts of smoke that produced mild ($n = 5$), moderate ($n = 5$), or severe ($n = 6$) smoke inhalation injury in a previous study (20). Measurements were made 24 h after smoke exposure, when changes in cardiopulmonary function showed a distinct dose response.

Time-related changes were studied in 26 sheep. Moderate smoke inhalation injury was produced in 20 sheep, and measurements were made 6, 12, 24, and 72 h after smoke exposure in groups of 5. Six uninjured sheep were used as controls.

In conducting the research described in this report, the investigators adhered to the Animal Welfare Act and other Federal statutes and regulations relating to animals and experiments involving animals and to the "Guide for the Care and Use of Laboratory Animals" [Department of Health, Education, and Welfare Publication no. (NIH) 85-23, revised 1985, Office of Science and Health Reports, DRR/NIH, Bethesda, MD 20892].

Smoke exposure. Sheep were intubated, anesthetized with methohexital sodium (9 mg/kg, Brevital, Eli Lilly, Indianapolis, IN), and insufflated with a standard dose of smoke to produce mild, moderate, or severe injury. The sheep model has been described in detail elsewhere (20), but in summary it enables dose-dependent injury by insufflating the lungs with a certain volume of smoke under general anesthesia and intubation. Smoke was produced by burning 10 disposable underpads (Hosposable, Bound Brook, NJ) in a smoke generator. The smoke generator was a 32-gallon metallic container equipped with an air inlet, a dampered chimney, a window, and a smoke outlet. The smoke was administered at ambient temperature to avoid thermal injury of the airway and contained 10–14% oxygen, 3–8% carbon dioxide, 0.7–2.2% carbon monoxide, and other combustion products but no cyanide. The experimental sheep were individually exposed to smoke with a tidal volume of 30 ml/kg and breath hold of 5 s followed by 10 successive ventilations with room air, which

were defined as 1 unit of smoke exposure. The time required per unit was ~50 s. Mild, moderate, and severe injuries were induced by exposing sheep to 3, 9, and 12 units of smoke, respectively.

The sheep started breathing spontaneously soon after smoke exposure and were extubated and housed in climate-controlled facilities (at 74–76°F and a relative humidity of 40–50%) until cardiopulmonary function and $\dot{V}_A/\dot{Q}$ distribution were measured.

Monitoring. Sheep were studied at 24 h after smoke inhalation for evaluation of severity-related changes and at 6, 12, 24, and 72 h after smoke exposure, in groups of five, for time-related alterations. Before the measurements, arterial, peripheral, and central venous lines, a Swan-Ganz catheter (7-Fr, American Edwards Laboratories, Irvine, CA), and an esophageal balloon were inserted after induction of general anesthesia and intubation. Anesthesia was induced with methohexital sodium and maintained with α-chloralose (0.05 g/kg, Calbiochem, La Jolla, CA), and the sheep were paralyzed with pancuronium bromide (0.03–0.04 mg/kg, Pavulon, Organon Pharmaceuticals, West Orange, NJ) (2). Chloralose and pancuronium bromide were administered with one-half of the initial dose as needed to maintain anesthetized and paralyzed conditions. After the placement of catheters, the animals were positioned prone and artificially ventilated. A volume-limited ventilator (Bear 2, Bear Medical Systems, Riverside, CA) with a tidal volume of 15 ml/kg was used at a respiratory rate of 12 breaths/min and inspired oxygen concentration ($F_{I_{O_2}}$) of 21% (room air). Sigh ventilation with a tidal volume of 21 ml/kg was applied every 3 min to prevent atelectasis. Lactated Ringer solution was continuously infused at a rate of 1 ml·kg weight^{-1}·h^{-1}.

Central venous pressure and pulmonary arterial pressure were monitored with Statham P23Db transducers (Statham Instruments, Oxnard, CA), and systemic arterial pressure was monitored with a Hewlett-Packard 1290A quartz transducer (Hewlett-Packard, Waltham, MA). Respiratory indexes were monitored with a pneumotachograph (model 17212, Gould) for flow rate and tidal volume and a differential transducer (MP-451, Validine Engineering, Northridge, CA) for transpulmonary pressure. The position of the esophageal balloon was adjusted to reflect the negative intrathoracic pressure, and transpulmonary pressure was taken as the pressure gradient between the connector site of the endotracheal tube to the respiratory circuit and the esophageal balloon. These cardiopulmonary indexes were recorded continuously on two Hewlett-Packard four-channel recorders (model 7754A). Cardiac output was measured in triplicate by thermodilution technique (cardiac output computer, model 9520A, American Edwards Laboratories). Blood gas analysis was performed by using an IL 1303 pH/blood gas analyzer and IL 282 CO-oximeter (Instrumentation Laboratories, Lexington, MA). Thermodilution cardiac output and arterial (Pa_{O_2}) and mixed venous ($P\bar{v}_{O_2}$) blood gas levels were measured every 30 min. The values measured at 2 h were taken as representative values when they were judged to be in stable condition from the traces of blood pressure, heart rate, and airway pressure as well as serial measurement of Pa_{O_2} and cardiac output. The sigh modality was discontinued 30 min before the measurement of $\dot{V}_A/\dot{Q}$, which requires gas-exchange equilibrium in the lung.

Static compliance of the lung was calculated from the following equation at end inflation (3): compliance = volume change/transpulmonary pressure.

Transpulmonary pressure (mouth pressure − intrapleural pressure) was measured with the differential transducer. Measurement was made at end inflation by placing a prolonged pause before exhalation.

Pulmonary resistance (RL) was calculated from the following equation: RL = (mouth pressure − intrapleural pressure)/flow rate. RL includes airway resistance plus pulmonary tissue resistance (3).

All the physiological measurements including MIGET were made under mechanical ventilation with $F_{I_{O_2}}$ of 0.21.

Necropsies were performed on all sheep killed at the end of the experiments for histological examination.

MIGET. MIGET was performed according to the method described by Wagner et al. (26, 28) with some modifications. Modifications included replacement of ethane, as originally employed, with krypton and the use of GC-mass spectrometry (MS) instead of GC with flame ionization and electron-capture detectors.

The six gases used in this study were sulfur hexafluoride (SF_6), krypton, cyclopropane, diethyl ether, halothane, and acetone. Ethane was replaced with krypton because trace levels of ethane were detected in expired gas in some sheep, probably derived from fermentation in the rumen (7). Ethane and krypton have almost the same solubility and are equivalent for the MIGET. However, the use of krypton necessitated mathematical compensation to correct the blood and expired gas samples for the natural occurrence of krypton (1.1×10^{-6} vol/vol) in ambient air. Correction was made by subtracting the krypton level in the air ($P_{Kr,0}$, measured) from that measured in expired gas samples ($PE_{Kr,m}$; $PE_{Kr} = PE_{Kr,m} - P_{Kr,0}$). For blood samples, blood krypton level ($P_{Kr,1}$) was measured by using krypton-free nitrogen for extraction, as described in the original MIGET method, and then the contribution from the atmospheric krypton, i.e., the dissolved krypton ($P_{Kr,2}$) from the atmosphere, was subtracted (*Eq. 1*). $P_{Kr,2}$ was calculated by performing mass balance by using $P_{Kr,0}$ and measured krypton solubility (S) according to *Eq. 2*. Use of corrected krypton values in the standard MIGET program is evaluated in the APPENDIX

$$P_{Kr,blood} = P_{Kr,1} - P_{Kr,2} \quad (1)$$

$$P_{Kr,2}(V_{liquid} \cdot K \cdot S + V_{gas}) = P_{Kr,0} \cdot V_{liquid} \cdot K \cdot S \quad (2)$$

where PE_{Kr} is the corrected expired krypton level used for $\dot{V}_A/\dot{Q}$ computation; $P_{Kr\,blood}$ is the corrected blood krypton level used to recover $\dot{V}_A/\dot{Q}$ distribution; K is (barometric pressure − saturated water vapor pressure)/100; V_{liquid} is the volume of liquid (blood + heparin) in the syringe; S is the solubility of krypton; and V_{gas} is the volume of gas added for extraction.

Measurement of the inert gases was made with a Hewlett-Packard GC-MS model 5985. GC requires two different detectors, an electron-capture detector for SF_6 and a flame-ionization detector for the other gases. Krypton is not measurable at trace levels with any detector except a MS. A glass column (1/4-in. OD × 6 ft) filled with Poropak-T (mesh 80/100) was employed by using helium as the carrier gas at a flow rate of 47 ml/min. Column temperature was maintained at 160°C. The MS was tuned with an electron energy of 30 V, an electron-multiplier voltage of 2,200 V, and a source temperature of 200°C. Detection was performed by single-ion monitoring for masses 127 (SF_6), 84 (krypton), 42 (cyclopropane), 74 (diethyl ether), 198 (halothane), and 58 (acetone).

Preliminary examinations demonstrated that the detector was sufficiently linear and reproducible over biological concentrations for in vitro and in vivo measurements. Linearity was tested by using a least squares linear regression analysis. The square of the coefficient of correlation (r^2) between peak area and concentration (vol/vol) ranged from 0.9988 (cyclopropane, acetone) to 0.9999 (diethyl ether) (Fig. 1). Reproducibility,

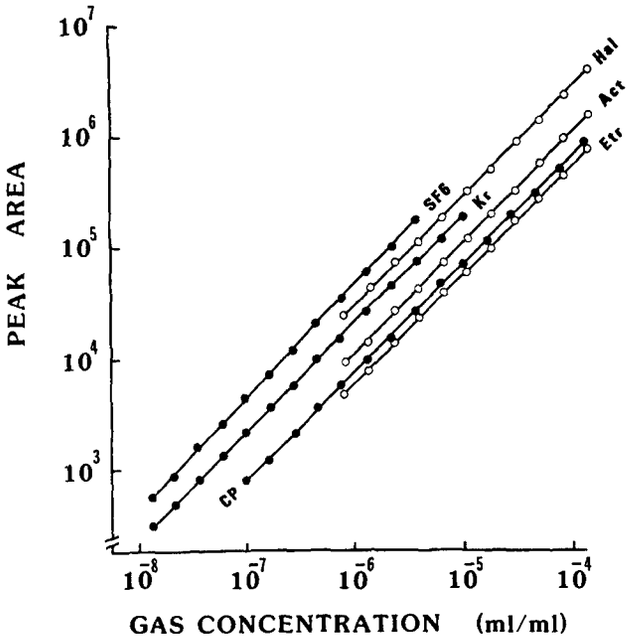

Fig. 1. Linearity of gas chromatography-mass spectrometry over physiological range for 6 gases: sulfur hexafluoride (SF_6), krypton (Kr), cyclopropane (CP), halothane (Hal), diethyl ether (Etr), and acetone (Act). Gases were separated into 2 groups for dilution study (23). SF_6, Kr, and CP were diluted together, and Hal, Etr, and Act were diluted together. Scale is log-log. Linearity was tested by using least squares linear regression analysis. Square of coefficient of correlation (r^2) between peak area and concentration (vol/vol) ranged from 0.9988 (CP, Act) to 0.9999 (Etr).

expressed as the coefficient of variation (means ± SD) of the GC-MS method for gas phase measurement, ranged from 0.46 (acetone) to 0.97% (SF_6). The reproducibility in blood samples ranged from 3.1 (halothane) to 5.2% (SF_6), values that are comparable to those measured with the standard GC detectors: 5.7% for SF_6 with electron-capture detector and 2–3% for the other gases with flame-ionization detector (25, 26).

Solubilities of the inert gases were measured individually in each animal according to the original method (26). Solubilities of SF_6, krypton, cyclopropane, halothane, ether, and acetone were 0.00090 ± 0.00015, 0.00908 ± 0.00175, 0.0583 ± 0.0137, 0.268 ± 0.0353, 1.408 ± 0.117, and 50.2 ± 7.15 (SD) ml gas·100 ml blood^{-1}·mmHg^{-1} at 40°C, respectively. The solubility of krypton ranged from 0.0061 to 0.0118 ml gas·100 ml blood^{-1}·mmHg^{-1}, but there was no significant correlation with the hematocrit ($r^2 = 0.02$, $P = 0.33$).

Ninety minutes after the induction of anesthesia, the sigh modality and lactated Ringer infusion were discontinued and a lactated Ringer solution containing the six inert gases was infused at a rate of 0.1 ml·kg^{-1}·min^{-1}. After 30 min, when equilibrium of gas exchange was reached, arterial and mixed venous blood were drawn anaerobically into preweighed heparinized syringes (30 ml, matched, glass, Becton-Dickinson) simultaneously. Mixed expired gas was taken from a temperature-controlled copper coil (OD = 4.49 cm, length = 6,400 cm) ~1 min after blood sampling, compensating for the delay in the mixing chamber. Blood and expired-gas samples were taken in duplicate and were analyzed immediately by MS. Representative $\dot{V}_A/\dot{Q}$ distributions were then calculated on a VAX-11780 (Digital Equipment) computer. The original program, developed for use with MIGET employing a GC, was modified only for subroutines that handle error terms to fit for our system (computer display of peak area and experimental error). In principle, the duplicate data sets were used to average the $\dot{V}_A/\dot{Q}$ parameters (i.e., moments, predicted Pa_{O_2}, and so on). If residual sums of squares of the best fit exceeded 16.8, the data were not used because the chance of this happening is only 1% (see χ^2 table for degree of freedom of 6) when residual sums of squares of the best fit are >16.8 (15). To avoid the effect of acetone in the heparin, we used heparin that was reported to be free of acetone (heparin sodium injection, Upjohn, Kalamazoo, MI) and tested a vial from each lot before use to confirm it to be free of acetone (14).

Statistical analysis. Data were displayed as means ± SD. Multiple comparisons of cardiopulmonary indexes were made by one-way analysis of variance (Tukey's and Bonferroni's tests) (6). $\dot{V}_A/\dot{Q}$ results were examined by multivariate analysis to compare fractional blood flow to the four major compartments among different groups (see Figs. 3 and 5, Tables 3 and 5) because each fractional blood flow cannot be independent from the others and, as such, univariate analysis will cause the probability of type I error to be higher for each analysis than the selected level of significance used (17). Significance was assigned when $P < 0.05$.

RESULTS

The animals regained spontaneous breathing soon after smoke insufflation, and breathing was supported by an Ambu-bag until they were extubated. The sheep usually started walking within 10 min after smoke exposure. Peak carboxyhemoglobin (HbCO) levels immediately after smoke exposure were 51.4 ± 9.8% in the mild-injury group, 64.4 ± 6.8% in the moderate-injury group, and 73.2 ± 5.7% in the severe-injury group (Table 1). In the time-related study groups, peak HbCO levels ranged from 61.2 ± 11.7 to 67.2 ± 3.0%. At 6 h after exposure, HbCO levels were 20.2 ± 2.3%, suggesting that the cardiopulmonary indexes at this period are more or less affected by HbCO (Table 1). Sheep exposed to smoke exhibited symptoms such as coughing, wheezing, and frothing. All sheep were able to breath spontaneously and stand unassisted before measurements were made.

Severity-related alterations. Table 2 summarizes cardiopulmonary indexes at 24 h. Pa_{O_2} became progressively lower as the severity increased. Moderate- and severe-injury groups had significantly lower Pa_{O_2} values than the control group. $P\bar{v}_{O_2}$, pH, arterial P_{CO_2} (Pa_{CO_2}), heart rate, RL, peak inspiratory pressure, and static compliance showed severity-related changes, and

Table 1. *Blood carboxyhemoglobin levels*

	Peak	At Measurement
Severity-related study		
Control	3.8 ± 1.4	5.7 ± 1.7
Mild-injury group	51.4 ± 9.8	5.2 ± 0.94
Moderate-injury group	64.4 ± 6.8	5.1 ± 1.4
Severe-injury group	73.2 ± 5.7	5.8 ± 1.3
Time-related study		
Control	4.0 ± 1.3	5.9 ± 1.5
6-h group	67.2 ± 3.0	20.2 ± 2.3
12-h group	61.5 ± 8.7	7.4 ± 1.4
24-h group	64.5 ± 5.6	5.8 ± 0.96
72-h group	61.2 ± 11.7	5.0 ± 0.87

Values are means ± SD. Peak carboxyhemoglobin (HbCO; in %) was measured in venous samples at end of smoke exposure. At measurement, HbCO was measured in arterial samples at allocated time. HbCO levels of arterial blood are 1–3% higher than those of simultaneously drawn venous samples.

Table 2. *Severity-related changes in cardiopulmonary indexes at 24 h*

	Control	Mild Injury	Moderate Injury	Severe Injury
Pa_{O_2}, Torr	101 ± 6.5	86.8 ± 2.8	66.0 ± 10.1‡	46.5 ± 8.6‡
$P\bar{v}_{O_2}$, Torr	37.8 ± 6.0	40.2 ± 2.5	35.0 ± 5.1	24.5 ± 4.9‡
Pa_{CO_2}, Torr	31.0 ± 4.9	29.9 ± 3.2	40.9 ± 3.2	47.5 ± 14*
pH	7.534 ± 0.045	7.570 ± 0.054	7.505 ± 0.044	7.420 ± 0.080*
Cardiac index, l/min	3.8 ± 0.21	4.2 ± 0.65	5.10 ± 1.49*	3.80 ± 1.13
Heart rate, beats/min	149 ± 15.5	149 ± 11.7	194 ± 14.4	200 ± 39.7*
$\bar{P}pa$, Torr	12.0 ± 3.7	17.2 ± 3.0	18.6 ± 5.4	20.8 ± 6.3†
PI_{peak}, cmH_2O	5.4 ± 1.4	6.8 ± 2.1	10.6 ± 3.0	17.1 ± 4.7‡
Cst, ml/cmH_2O	169 ± 24	130 ± 26	94 ± 35	52 ± 30‡
RL, $cmH_2O \cdot s \cdot l^{-1}$	11.6 ± 2.5	15.8 ± 5.8	23.8 ± 9.6	52.2 ± 30.0‡

Values are means ± SD. Pa_{O_2}, arterial P_{O_2}; $P\bar{v}_{O_2}$, mixed venous P_{O_2}; Pa_{CO_2}, arterial P_{CO_2}; $\bar{P}pa$, mean pulmonary arterial pressure; PI_{peak}, peak inspiratory pressure; Cst, static compliance calculated as described in text; RL, pulmonary resistance calculated as described in text. Only significant difference from control is shown, although Bonfferoni test was made for all possible pairs of means, i.e., for 6 comparisons. *$P < 0.05$, †$P < 0.10$, ‡$P < 0.01$, significantly different from control [1-way analysis of variance (ANOVA)].

the changes were significant in the severely injured group. However, the severe-injury group showed no significant changes compared with the control in cardiac index ($P > 0.10$), pulmonary arterial pressure ($0.10 > P > 0.05$), total peripheral resistance index ($P > 0.10$), or pulmonary vascular resistance index ($P > 0.10$).

Typical $\dot{V}_A/\dot{Q}$ patterns after various levels of smoke inhalation injury are shown in Fig. 2. Controls (Fig. 2*A*) had sharp peaks of ventilation and perfusion at $\dot{V}_A/\dot{Q} = 1$, suggesting good $\dot{V}_A/\dot{Q}$ matching, whereas bimodal ventilation distribution would primarily be attributable to relatively large tidal volume setting of the ventilator. Figure 2*B* shows an example of mildly injured animals that had minimal hypoxemia (Pa_{O_2} of 85 Torr), but peaks of ventilation and perfusion near one were wider and true shunt ($\dot{V}_A/\dot{Q} = 0$) was observed. Moderate injury (Fig. 2*C*) produced further $\dot{V}_A/\dot{Q}$ mismatching as hypoxemia became more severe with development of low $\dot{V}_A/\dot{Q}$ ($0 < \dot{V}_A/\dot{Q} < 0.1$). In this example, 6.2% of the cardiac output perfused unventilated parts of the lung (true shunt). In the severely injured sheep (Fig. 2*D*), the low $\dot{V}_A/\dot{Q}$ developed further and 42% of the cardiac output perfused the low $\dot{V}_A/\dot{Q}$, whereas there was little increase in shunt flow in this example.

$\dot{V}_A/\dot{Q}$ patterns of blood flow were bimodal distribution in almost all the animals exposed to moderate and severe injuries. We did not observe any wide unimodal blood flow distribution pattern extending over normal and low $\dot{V}_A/\dot{Q}$ compartments that would explain moderate or severe hypoxia, whereas relatively wide unimodal distribution was frequently observed in mildly hypoxic sheep, as shown in the example of Fig. 2*B*.

Severity-related changes in $\dot{V}_A/\dot{Q}$ values are summarized in Table 3. $\dot{V}_A/\dot{Q}$ distribution was divided into four major compartments: true shunt ($\dot{V}_A/\dot{Q} = 0$), low $\dot{V}_A/\dot{Q}$ ($0 < \dot{V}_A/\dot{Q} < 0.1$), normal $\dot{V}_A/\dot{Q}$ ($0.1 < \dot{V}_A/\dot{Q} < 10$), and high $\dot{V}_A/\dot{Q}$ ($\dot{V}_A/\dot{Q} > 10$) (Fig. 3). Fractional blood flows to the four compartments are shown as percent cardiac output. In the controls, 98.4% of the cardiac output went to the normal $\dot{V}_A/\dot{Q}$ compartment. Blood flow to the normal compartment decreased progressively as the injury became more severe, whereas flows to the shunt and low $\dot{V}_A/\dot{Q}$ compartment increased reciprocally. These changes were significant in the moderate- and severe-injury groups. The high $\dot{V}_A/\dot{Q}$ compartment showed no significant changes.

Table 3 also shows progression of the overall $\dot{V}_A/\dot{Q}$ mismatch (dispersion) expressed as the second moments of ventilation and blood flow distributions, log $SD_{\dot{V}}$ and log $SD_{\dot{Q}}$, respectively (9, 23). The dispersion index of perfusion (log $SD_{\dot{Q}}$) was elevated significantly in the moderate- and severe-injury groups as the center of the perfusion mean $\dot{Q}$ shifted to the left. There were no significant differences in mean $\dot{V}$, log $SD_{\dot{V}}$, or dead space (dead space divided by tidal volume) ($P > 0.10$).

Time-related alterations in sheep with moderate injury. Changes in cardiopulmonary indexes are shown in Table 4. Pa_{O_2} became progressively lower with time and was significantly lower after 12 h, but the decrease in $P\bar{v}_{O_2}$ became significant only at 72 h. The decrease in static compliance and increase in RL and pulmonary arterial pressure were significant at 72 h, whereas the increase in peak inspiratory pressure reached a significant level at 24 h. Cardiac index, heart rate, pH, Pa_{CO_2}, dead space, total peripheral resistance index, and pulmonary vascular index showed no significant changes ($P > 0.10$).

$\dot{V}_A/\dot{Q}$ changes with time after moderate inhalation injury are depicted in Fig. 4. Blood flow to the normal $\dot{V}_A/\dot{Q}$ compartment decreased with time, and flow to the low $\dot{V}_A/\dot{Q}$ compartment increased reciprocally. These changes reached significant levels at 72 h. Increase in the true shunt was observed in some animals but was not a consistent finding ($P > 0.10$). Blood flow to the high $\dot{V}_A/\dot{Q}$ compartment did not change at all ($P > 0.10$).

Temporal changes in the dispersion indexes are also summarized in Table 5. Dispersion of blood flow (log $SD_{\dot{Q}}$) increased significantly with time as hypoxemia progressed while the center of the distribution, indexed by mean $\dot{Q}$, shifted to the left. There were no significant differences in shunt flow, mean $\dot{Q}$, mean $\dot{V}$, log $SD_{\dot{V}}$, or dead space ($P > 0.10$).

To evaluate the relative contribution of the true shunt and the low $\dot{V}_A/\dot{Q}$ to the disturbance of oxygenation, relationships between Pa_{O_2} and shunt flow (S in Fig. 3; %cardiac output), flow to the low $\dot{V}_A/\dot{Q}$

compartment (L in Fig. 3) and shunt plus low $\dot{V}_A/\dot{Q}$ compartment (S+L in Fig. 5) were studied with linear regression analysis. Blood flow to L had good correlation with measured Pa_{O_2} (Pa_{O_2} = 92.2 − 106.6L; r^2 = 0.692; $P < 0.01$; n = 47), whereas Pa_{O_2} and S did not show close correlation (r^2 = 0.228). On the other hand, S+L showed significant correlation with Pa_{O_2} (Pa_{O_2} = 93.9 − 94.7(S+L); r^2 = 0.749; $P < 0.01$; n = 47; Fig. 5). These results suggest that development of low $\dot{V}_A/\dot{Q}$ is the primary mechanism of hypoxia after smoke inhalation injury.

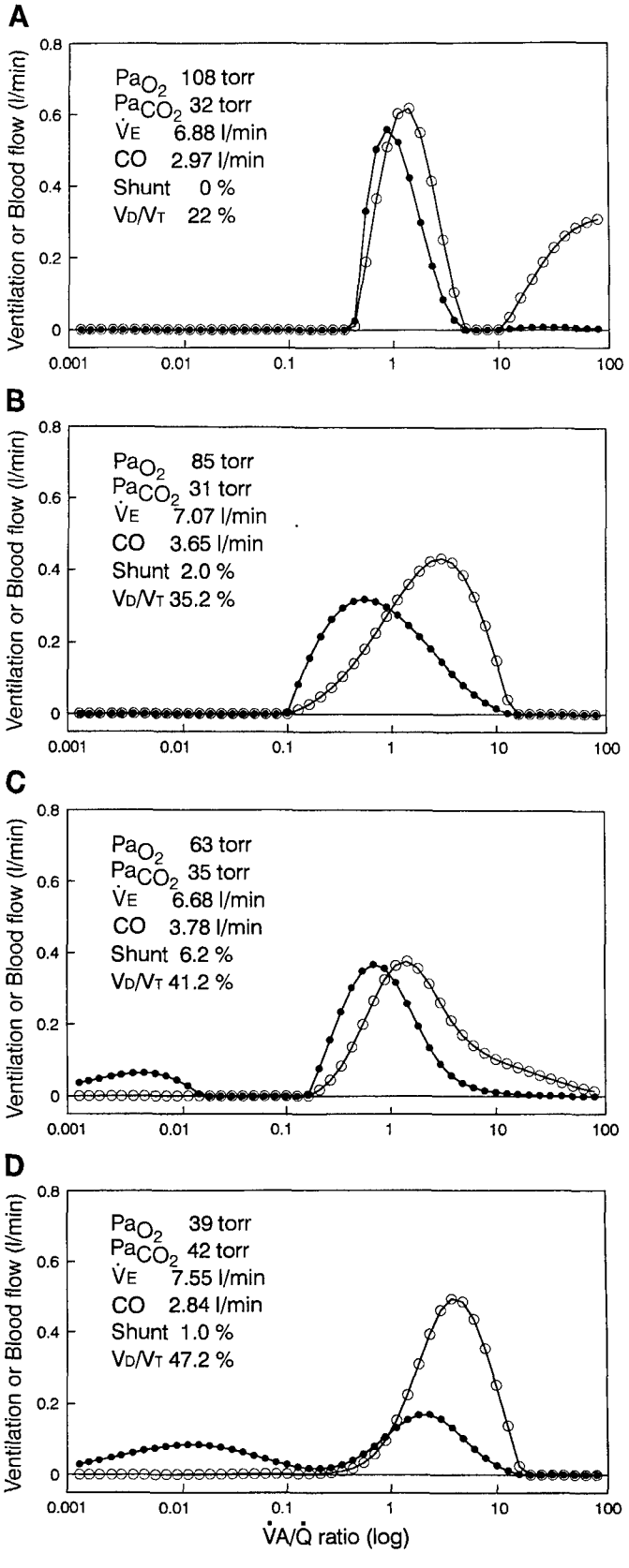

Fig. 2. Typical ventilation-perfusion ratio ($\dot{V}_A/\dot{Q}$) distributions at 24 h after exposure to various extents of smoke injury. ●, Blood flow; ○, ventilation. *A*: control animals had sharp peaks of ventilation and perfusion at $\dot{V}_A/\dot{Q}$ = 1, whereas bimodal ventilation distribution would primarily be attributable to relatively large tidal volume setting. *B*: peaks of ventilation and perfusion became broader and true shunt ($\dot{V}_A/\dot{Q}$ = 0) was observed in a mildly injured example. *C*: moderate injury produced further $\dot{V}_A/\dot{Q}$ mismatch with development of low $\dot{V}_A/\dot{Q}$ ($0 < \dot{V}_A/\dot{Q} < 0.1$) and moderate true shunt. *D*: in a severely injured sheep, low $\dot{V}_A/\dot{Q}$ developed further, but true shunt was minimal. Note that illustrations correspond to 4 different representative sets of data derived from a single animal in each category studied. Pa_{O_2}, arterial P_{O_2}; Pa_{CO_2}, arterial P_{CO_2}; $\dot{V}_E$, minute ventilation; CO, cardiac output; V_D/V_T, dead space (V_D)-to-tidal volume (V_T) ratio. See text for details.

Table 3. *Severity-related changes in $\dot{V}_A/\dot{Q}$ indexes at 24 h*

	Control	Mild Injury	Moderate Injury	Severe Injury
Shunt[a]	0.4 ± 0.5	0.5 ± 0.8	5.6 ± 5.5	11.7 ± 9.5[h]
Low $\dot{V}_A/\dot{Q}$[b]	0.4 ± 0.8	7.8 ± 7.9	17.6 ± 10.6[h]	36.9 ± 4.7[h]
Normal $\dot{V}_A/\dot{Q}$[c]	98.4 ± 0.9	91.3 ± 7.2	76.4 ± 9.3[h]	50.8 ± 9.8[h]
High $\dot{V}_A/\dot{Q}$[d]	0.8 ± 0.4	0.5 ± 0.4	0.3 ± 0.4	0.6 ± 0.9
Mean $\dot{Q}$[e]	0.96 ± 0.21	0.73 ± 0.23	0.43 ± 0.33[i]	0.23 ± 0.12[j]
Log $SD_{\dot{Q}}$[f]	0.76 ± 0.14	1.37 ± 0.42	1.75 ± 0.48[i]	2.52 ± 0.37[j]
Mean $\dot{V}$[e]	3.35 ± 1.41	2.42 ± 0.59	2.20 ± 0.46	3.70 ± 2.42
Log $SD_{\dot{V}}$[f]	1.40 ± 0.56	1.14 ± 0.30	1.05 ± 0.29	1.09 ± 0.43
V_D/V_T[g]	33.9 ± 7.0	39.3 ± 3.1	41.7 ± 4.9	45.2 ± 14.9

Values are means ± SD. $\dot{V}_A/\dot{Q}$, ventilation-perfusion ratio. [a]Blood flow ($\dot{Q}$) to true shunt ($\dot{V}_A/\dot{Q} = 0$); [b]$\dot{Q}$ to low $\dot{V}_A/\dot{Q}$ compartment ($0 < \dot{V}_A/\dot{Q} < 0.1$); [c]$\dot{Q}$ to normal $\dot{V}_A/\dot{Q}$ compartment ($0.1 < \dot{V}_A/\dot{Q} < 10$); [d]$\dot{Q}$ to high $\dot{V}_A/\dot{Q}$ compartment ($10 < \dot{V}_A/\dot{Q}$); [a–d] are expressed as percentage of cardiac output. [e]Mean $\dot{Q}$ (l/min) or ventilation ($\dot{V}$; l/min) on logrithmic scale (9); [f]second moment of $\dot{Q}$ distribution ($logSD_{\dot{Q}}$) or ventilation distribution ($logSD_{\dot{V}}$) (9, 23); [g]dead space [dead space (V_D)-to-tidal volume (V_T) ratio] obtained from multiple inert gas elimination technique (MIGET) expressed as % minute ventilation; [h]significant change ($P < 0.01$) from control level by multivariate analysis (see text for details); [i]$P < 0.05$; [j]$P < 0.01$ significantly different from control (1-way ANOVA).

Histological changes at 24 h after mild smoke inhalation injury (Fig. 6) included sloughed respiratory epithelial cells and inflammatory cells occluding the airway. Early vascular congestion and septal thickening extending from the obstructed airway were noted. The alveolar spaces were essentially normal. These observations were compatible with our previous reports (12, 20).

Finally, to show the reliability of the experimental procedures, some basic indexes measured by standard method were compared with those derived from the $\dot{V}_A/\dot{Q}$ distribution. Measured Pa_{O_2} and estimated Pa_{O_2} from the $\dot{V}_A/\dot{Q}$ distribution for the 47 sheep in this study showed good correlation with r^2 = 0.73 and $P < 0.01$ [Pa_{O_2} (predicted) = 19.3 + 0.72Pa_{O_2} (measured)]. There was no significant difference between the values of measured P_{O_2} (78.2 ± 19.5 Torr) and predicted P_{O_2} (75.4 ± 16.3 Torr) by paired t-test (P = 0.063, n = 47

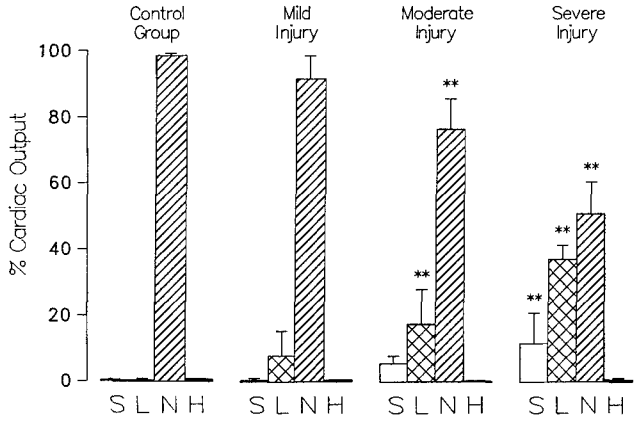

Fig. 3. Severity-related changes in fractional blood flow 24 h after smoke inhalation injury. Values are means ± SD. $\dot{V}_A/\dot{Q}$ distribution was divided into 4 major compartments: true shunt (S; $\dot{V}_A/\dot{Q} = 0$); low $\dot{V}_A/\dot{Q}$ (L; $0 < \dot{V}_A/\dot{Q} < 0.1$); normal $\dot{V}_A/\dot{Q}$ (N; $0.1 < \dot{V}_A/\dot{Q} < 10$); and high $\dot{V}_A/\dot{Q}$ (H; $10 < \dot{V}_A/\dot{Q}$). As blood flow to N decreased with increasing severity, blood flow to S and L increased reciprocally. **Significant change ($P < 0.01$) from control level by multivariate analysis.

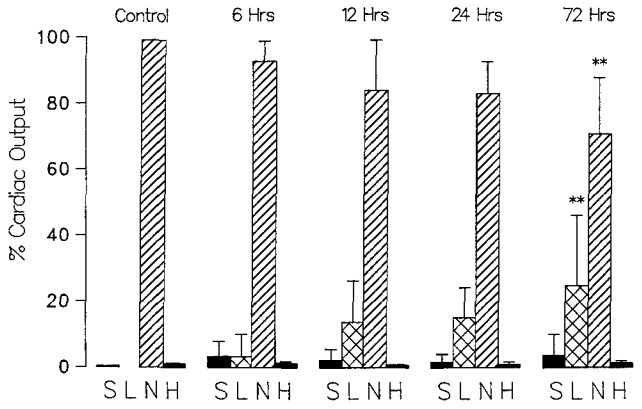

Fig. 4. Temporal changes in fractional blood flow after moderate smoke inhalation injury. Values are means ± SD. See Fig. 3 for definitions. Blood flow to N decreased and was recruited to L, where it reached a significant level at 72 h. Increased blood flow to S was not a consistent finding and did not show significance at any time. **Significant change ($P < 0.01$) from control level by multivariate analysis.

pairs), indicating that hypoxemia is adequately explained by $\dot{V}_A/\dot{Q}$ mismatch mechanism. Cardiac output (CO in Fig. 2*A*) measured by thermodilution method and MIGET-derived cardiac output for the 47 sheep in this study also showed fairly good correlation [CO (inert gas) = 0.97 + 0.75CO (measured with Swan-Ganz catheter method), $r^2 = 0.58$, $P < 0.01$].

DISCUSSION

Main findings. Severity-related and time-related changes after smoke inhalation injury were very similar. Progressive hypoxemia, lower lung compliance, and higher airway resistance were noted as the severity of injury increased. The observed hypoxemia and changes in ventilatory mechanics suggest substantial changes in $\dot{V}_A/\dot{Q}$ distribution, findings confirmed by the MIGET. The changes in $\dot{V}_A/\dot{Q}$ distribution after smoke inhalation injury, in terms of severity-related and time-related progression, were characterized by development of low $\dot{V}_A/\dot{Q}$ ($0 < \dot{V}_A/\dot{Q} < 0.1$), explaining the observed hypoxemia. Increase in true shunt ($\dot{V}_A/\dot{Q} = 0$) was not a consistent finding and was statistically significant only in the severely injured group (Fig. 3), although occasional individual animals in other groups developed moderate shunt flow. These results suggest that the development of hypoxemia after smoke inhalation injury was primarily attributable to increased perfusion of the low $\dot{V}_A/\dot{Q}$.

Critique of methods. Validity and limitations of the method we employed to compensate for the atmospheric krypton were evaluated in the APPENDIX. In summary, prior correction by subtraction of partial pressure of inspirate from arterial partial pressure, mixed expired gas partial pressure, and mixed venous partial pressure produced no error in normal or injured lungs of animals breathing room air (Table 6).

There might also be an argument that, even if the animals are producing ethane, measurement of the retention and excretion of the naturally produced ethane would be enough and that any methane production could be separated from ethane on a GC. However, natural ethane is not usable in this particular situation due to lack of separation from methane because both ethane and methane were detected in expired gas. Furthermore, when we say ethane was detected in expired gas, what we are really saying is that a peak appeared where ethane normally appears. We cannot be certain that this is ethane as opposed to some other

Table 4. *Time-related changes in selected cardiopulmonary indexes*

		Time, h			
	Control	6	12	24	72
Pa_{O_2}, Torr	101 ± 6.3	89.7 ± 9.2	78.0 ± 12.6†	68.8 ± 9.2†	63.5 ± 11.6†
$P\bar{v}_{O_2}$, Torr	38.7 ± 4.0	34.0 ± 2.5	34.2 ± 2.4	33.8 ± 3.3	32.6 ± 2.0*
Pa_{CO_2}, Torr	34.1 ± 4.1	32.2 ± 2.8	33.8 ± 5.1	33.8 ± 3.3	37.3 ± 9.3
pH	7.516 ± 0.023	7.480 ± 0.046	7.544 ± 0.031	7.524 ± 0.035	7.504 ± 0.073
Cardiac index, l/min	4.10 ± 0.72	4.8 ± 0.83	4.00 ± 0.89	4.00 ± 0.55	4.5 ± 1.40
Heart rate, beats/min	157 ± 21.3	167 ± 31.6	168 ± 22.8	175 ± 9.4	166 ± 26.7
$\bar{P}pa$, Torr	14.1 ± 1.2	14.9 ± 4.8	18.5 ± 8.1	18.4 ± 4.7	23.4 ± 2.7*
$P_{I_{peak}}$, cmH_2O	4.5 ± 1.1	5.9 ± 0.8	8.6 ± 2.1	9.3 ± 3.6*	13.8 ± 3.6†
Cst, ml/cmH_2O	180 ± 49	138 ± 30	138 ± 55	110 ± 27	75 ± 22†
R_L, $cmH_2O \cdot s \cdot l^{-1}$	10.3 ± 2.3	12.4 ± 1.8	19.1 ± 10.5	19.4 ± 10.5	37.2 ± 14.0†

Values are means ± SD. Only significant difference from control is marked, although Bonferroni test was made for all possible pairs of means, i.e., for 10 comparisons. *$P < 0.05$, †$P < 0.01$, significantly different from control (1-way ANOVA).

Table 5. *Time-related changes in $\dot{V}_A/\dot{Q}$ indexes*

	Control	Time, h 6	12	24	72
Shunt, %cardiac output[a]	0.3 ± 3.7	3.3 ± 4.9	2.2 ± 3.6	1.6 ± 2.7	3.6 ± 6.7
Low $\dot{V}_A/\dot{Q}$, %cardiac output[b]	0	3.2 ± 7.1	13.6 ± 12.8	14.9 ± 9.4	24.6 ± 21.4[h]
Normal $\dot{V}_A/\dot{Q}$, %cardiac output[c]	98.7 ± 0.4	92.1 ± 6.3	83.5 ± 15.3	82.5 ± 9.8	70.4 ± 17.2[h]
High $\dot{V}_A/\dot{Q}$, %cardiac output[d]	1.1 ± 0.5	1.3 ± 0.8	0.8 ± 0.3	0.9 ± 1.0	1.4 ± 0.9
Mean $\dot{Q}$, l/min[e]	0.90 ± 0.24	0.68 ± 0.15	0.54 ± 0.24	0.53 ± 0.26	0.48 ± 0.43
Log SD_Q[f]	0.62 ± 0.06	1.02 ± 0.39	1.70 ± 0.62[i]	1.78 ± 0.53[i]	1.85 ± 0.77[j]
Mean $\dot{V}$, l/min[e]	3.86 ± 1.37	4.27 ± 2.28	2.84 ± 0.79	3.56 ± 1.93	3.95 ± 1.00
Log $SD_{\dot{V}}$[f]	1.75 ± 0.47	1.63 ± 0.39	1.18 ± 0.43	1.26 ± 0.47	1.20 ± 0.44
V_D/V_T, %minute ventilation[g]	32.9 ± 9.3	24.5 ± 8.1	31.5 ± 8.9	35.9 ± 4.8	34.2 ± 5.2

Values are means ± SD. Symbols are defined as in Table 3.

hydrocarbon, and it may indeed be more than one gas, although we could avoid this problem partly by using MS as the detector. If this were the case, then with different gases having different solubilities, we would have a very complex situation to understand the behavior of the "ethane" peaks. All of these uncertainties are to be avoided by using krypton even if compensation for atmospheric krypton is necessary.

Pathophysiology. In reports of other acute respiratory insufficiencies, flows to the true shunt and to the low $\dot{V}_A/\dot{Q}$ make variable contributions to hypoxemia, reflecting the specific pathophysiology of the disease (27). Increased true shunt occurs in oleic acid-induced lung edema with little or no increase in the low $\dot{V}_A/\dot{Q}$ (5, 18, 24). Schoene et al. (18) reported that oleic acid-injured dogs developed significant shunt at postinjury *day 1*, with resolution of the shunt by *day 7*, whereas animals that developed suppurative bronchopneumonia after repeated bronchial lavage showed low $\dot{V}_A/\dot{Q}$. In the present study, inflammatory changes were observed in all the animals, and every animal with smoke inhalation showed a certain amount of perfusion to the low $\dot{V}_A/\dot{Q}$, although some were <5% of flow. Gas emboli produce hypoxemia mainly attributable to low $\dot{V}_A/\dot{Q}$ (10), whereas other acute injuries show combinations of shunt and low $\dot{V}_A/\dot{Q}$.

Changes in physiological dead space were somewhat similar to those of the shunt; some animals showed substantial increase in dead space and Pa_{CO_2}, but this

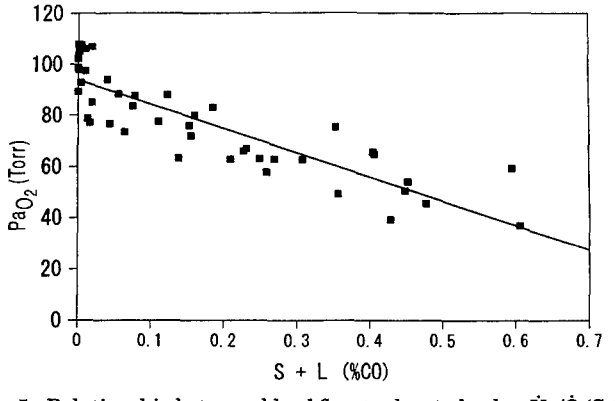

Fig. 5. Relationship between blood flow to shunt plus low $\dot{V}_A/\dot{Q}$ (S+L) and Pa_{O_2}. Blood flow to S+L showed excellent correlation with Pa_{O_2} (Pa_{O_2} = 93.9 − 94.7(S+L); r^2 = 0.749; $P < 0.01$); n = 47.

was not a consistent finding. Robinson et al. (16) have reported increased high $\dot{V}_A/\dot{Q}$ and dead space ventilation soon after smoke exposure, and Stollery et al. (22) suggested that increased dead space ventilation was responsible for respiratory failure at a later stage in a small subset of burn patients with inhalation injury. As Nunn (13) has pointed out, physiological interpretation at the higher end of the $\dot{V}_A/\dot{Q}$ scale is not as clear as that at the lower end. The high $\dot{V}_A/\dot{Q}$ cannot be evaluated without consideration of peak inspiratory pressure and Pa_{CO_2} because the measured perfusion of the high $\dot{V}_A/\dot{Q}$ is influenced by the tidal volume setting of the ventilator and such perfusion can occur even in control animals (Fig. 2). Peak inspiratory pressure was significantly elevated in the severely injured group at 24 h (Table 2) and in moderately injured animals at 24 and 72 h (Table 4), in many cases, with hypercapnia. In the present study, even though mean values did not change significantly, increased dead space and high $\dot{V}_A/\dot{Q}$ were observed in some of the moderately and severely injured animals and were associated with hypoxemia. These findings suggest that extensive small-airway occlusion caused by smoke inhalation diverted the inspired gas to alveoli with good compliance, leading to the increased high $\dot{V}_A/\dot{Q}$ and dead space ventilation. The findings could also be interpreted that the increased airway resistance facilitated both gas trapping and lung hyperinflation, thereby resulting in the development of regions with high $\dot{V}_A/\dot{Q}$ and increased dead space.

Development of the low $\dot{V}_A/\dot{Q}$, and especially of very low $\dot{V}_A/\dot{Q}$ ($\dot{V}_A/\dot{Q} \leq 0.01$; Fig. 2), characterized both severity-related and time-related $\dot{V}_A/\dot{Q}$ alterations after smoke inhalation injury. Such deviation of $\dot{V}_A/\dot{Q}$ from 1 (normal) to 0.01 (low) can be caused by either an increase in perfusion or a decrease in ventilation or probably by both. The $\dot{V}_A/\dot{Q}$ patterns suggest a disturbance of ventilation, such as airway constriction, obstruction by secretions, pulmonary edema, or some other cause of partial atelectasis, because a 100-fold increase in perfusion to a lung unit with normal $\dot{V}_A/\dot{Q}$ seems physiologically unlikely, if not impossible. This may be rephrased that it is unlikely that after moderate or severe injury 20–40% of the cardiac output goes to lung units that were virtually not perfused in control conditions. This interpretation of airway impair-

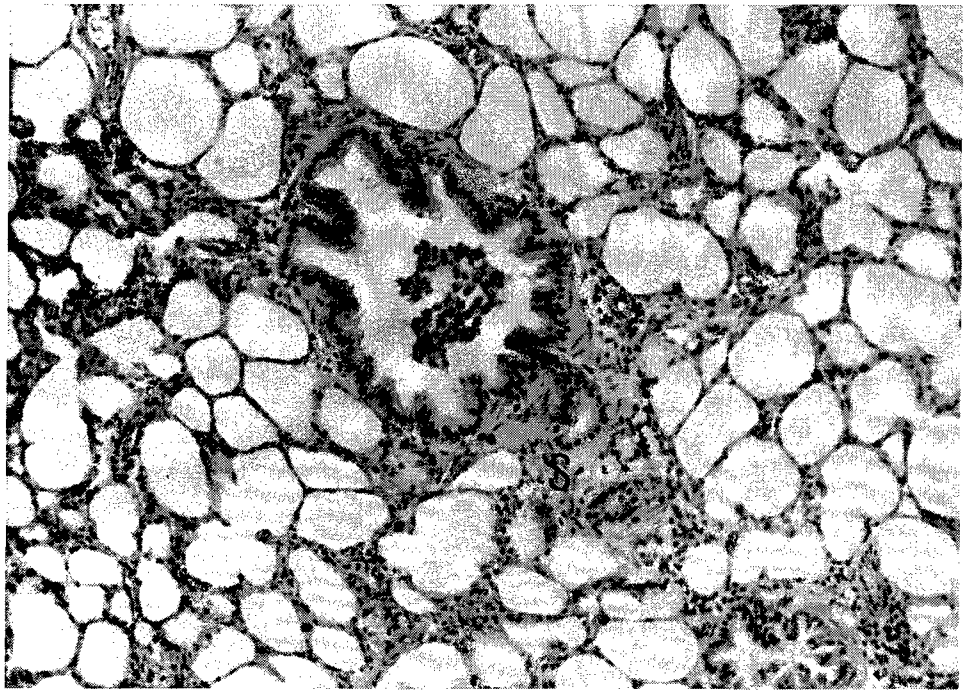

Fig. 6. Photomicrograph of a sheep lung 24 h after mild smoke inhalation injury. Sloughed respiratory epithelial cells and inflammatory cells are occluding an airway. Note early vascular congestion and septal thickening (S) extending from blocked airway. Alveolar spaces are essentially normal. Hematoxylin and eosin stain, ×1,020 = print magnification, ×325 = original magnification.

ment is consistent with histological findings (8, 12, 20; Fig. 6). Such low $\dot{V}_A/\dot{Q}$ is very unstable at higher inspiratory oxygen concentration ($F_{I_{O_2}}$) and is easily converted to true shunt, which should be noted in the respiratory management of patients with smoke inhalation injury (4, 19).

A previous study on $\dot{V}_A/\dot{Q}$ changes after smoke inhalation reported by Robinson et al. (16) was consistent with our results regarding the mechanism of hypoxemia. They measured $\dot{V}_A/\dot{Q}$ distribution in 5 patients with evidence of smoke inhalation (association of skin burn was not clear) at 24, 48, and 72 h after injury and in 10 rabbits (5 controls and 5 smoke inhalation) at 6 h after smoke exposure. They reported that early alterations of ventilation and perfusion resulted from increased high $\dot{V}_A/\dot{Q}$ and dead space ventilation, whereas late alterations were characterized by significantly increased perfusion of low $\dot{V}_A/\dot{Q}$ compartments and notably absent true intrapulmonary shunting. They did not describe very low $\dot{V}_A/\dot{Q}$ ($\dot{V}_A/\dot{Q} < 0.01$), which would be attributable to high $F_{I_{O_2}}$ (0.51 ± 0.07 at 24 h) employed to maintain Pa_{O_2} in the patients, although use of positive end-expiratory pressure was not clearly stated. They observed that predicted P_{O_2} values were systematically higher than measured ones in clinical cases and suggested increased postpulmonary shunt resulting from increased bronchial blood flow as the mechanism of such discrepancy. However, their speculation was based primarily on four measurements on *day 1*. They observed predicted P_{O_2} was higher than measured P_{O_2} in three of four cases, the probability of which would be 32%

Table 6. *Comparison between prior correction and correct kernel in 3 conditions of sheep data*

	Sheep 204, Normal ($F_{I_{O_2}} = 0.21$)		*Sheep 141*, injured ($F_{I_{O_2}} = 0.21$)		*Sheep 171*, injured ($F_{I_{O_2}} = 1.0$)	
	R_c (*Eq. A4*)	R_c (*Eq. A5*)	R_c (*Eq. A4*)	R_c (*Eq. A5*)	R_c (*Eq. A4*)	R_c (*Eq. A5*)
R_c (krypton)	0.04658	0.04666	0.35188	0.35196	0.44439	0.44480
E_c (krypton)	0.1779	0.01779	0.01409	0.01410	0.01836	0.01874
RSS	0.0696	0.0692	0.106	0.106	0.0178	0.0155
Log $SD_{\dot{Q}}$	0.96	0.96	2.59	2.59	1.21	1.10
Log $SD_{\dot{V}}$	0.78	0.78	0.74	0.74	0.83	0.85
Shunt (%)	0.0	0.0	0.1	0.1	37.9	38.4
$\dot{Q}$ in low $\dot{V}_A/\dot{Q}$ areas, %*	1.3	1.4	39.9	39.9	2.2	1.1
$\dot{V}$ in high $\dot{V}_A/\dot{Q}$ areas, %†	8.4	8.4	4.1	4.1	2.8	2.9
Dead space, %	13.0	12.9	45.1	45.1	53.5	53.6
Predicted Pa_{O_2}, Torr	97.0	97.0	49.6	49.6	83.6	83.0
$P_I/P\bar{v}$	0.0056	0.0056	0.0075	0.0075	0.062‡	0.062

R_c, corrected retention; R_c (*Eq. A4*), R_c according to *Eq. A4* (prior correction); R_c (*Eq. A5*), R_c according to *Eq. A5* (correct kernel); E_c, corrected excretion; E_c (*Eq. A4*), E_c according *Eq. A4;* E_c (*Eq. A5*), E_c according to *Eq. A5;* R_c (krypton), R_c of krypton; E_c (krypton), E_c of krypton; RSS, residual sum of squares of best fit to data (15); P_I, inspired partial pressure; $P\bar{v}$, mixed venous partial pressure; *fractional $\dot{Q}$ to low $\dot{V}_A/\dot{Q}$ ($0 < \dot{V}_A/\dot{Q} < 0.1$) compartment; †fractional $\dot{V}$ to high $\dot{V}_A/\dot{Q}$ ($\dot{V}_A/\dot{Q} > 10$) compartment; ‡way O_2 is produced from air by suppliers of 100% O_2 concentrates krypton severalfold, as these data show.

$[(4C1 + 4C0)/2^4 = (4 + 1)/16 = 0.31)]$. In this study, we did not see a statistically significant difference between predicted and measured Pa_{O_2} even with paired t-test ($P = 0.063$). Abdi et al. (1) measured bronchial blood flow in a sheep model of smoke inhalation and reported that bronchial circulation was 1% or less of cardiac output in normal condition but that it approached 5% of cardiac output after inhalation. Bronchial arterial occlusion in that sheep model resulted in reduced lung lymph flow and lung edema after inhalation injury, but oxygenation (Pa_{O_2}/FI_{O_2}) was not significantly different; in fact, those with occluded bronchial artery had a tendency to have a lower Pa_{O_2}/FI_{O_2} value. Therefore, it would not be necessary to introduce increased bronchial blood flow in the pathogenesis of hypoxemia after inhalation injury, whereas the possibility of diffusion limitation to oxygen or an increase of intrapulmonary oxygen consumption cannot totally be ignored. However, in this study hypoxemia was adequately explained by $\dot{V}_A/\dot{Q}$ mismatch mechanism.

In conclusion, $\dot{V}_A/\dot{Q}$ alterations after smoke inhalation injury were characterized by the development of low $\dot{V}_A/\dot{Q}$. Both severity-related and time-related progressive hypoxemia after inhalation of smoke were attributable to this change in the distribution of pulmonary ventilation and perfusion; increase in true shunt was not a consistent finding. Thus this $\dot{V}_A/\dot{Q}$ study suggests major impairment of the airway as the etiologic mechanism of hypoxemia after smoke inhalation injury.

APPENDIX

To evaluate validity and limitations of the method we employed to compensate for the atmospheric krypton, we analyzed the modification and then examined the possible error in three scenarios that reflect the conditions of our study fairly well.

The first question is, Does prior subtraction of partial pressure of krypton in the inspirate [P_I (krypton)] from arterial partial pressure (Pa), mixed expired gas partial pressure ($P\bar{E}$), and mixed venous partial pressure ($P\bar{v}$) allow use of the standard MIGET program by using the kernel retention (R) = excretion (E) = $\lambda/(\lambda + \dot{V}_A/\dot{Q})$, where λ is the partition coefficient of the gas, or should the kernel be modified to reflect P_I (krypton) > 0, thus using measured Pa, $P\bar{E}$ and $P\bar{v}$ without prior subtraction?

The correct kernel equation for P_I (krypton) > 0 is

$$R = E = \frac{\lambda + (\dot{V}_I/\dot{Q})\cdot(P_I/P\bar{v})}{\lambda + \dot{V}_A/\dot{Q}} \qquad (1A)$$

where $\dot{V}_I$ is the ventilation of krypton in the inspirate. This comes from mass balance considerations

$$\dot{V}_I \cdot P_I - \dot{V}_A \cdot P_A = \lambda\dot{Q}(Pa - P\bar{v})$$

where P_A is alveolar pressure and $\dot{Q}$ is blood flow.

If one uses the closely related kernel

$$R = E = \frac{\lambda + (\dot{V}_A/\dot{Q})\cdot(P_I/P\bar{v})}{\lambda + \dot{V}_A/\dot{Q}} \qquad (2A)$$

and then subtracts P_I from Pa, $P\bar{E}$, and $P\bar{v}$ to enable use of the usual MIGET algorithm, this correction would be algebraically perfect

$$R_c = \frac{Pa - P_I}{P\bar{v} - P_I} \qquad (3A)$$

$$= \frac{Pa/P\bar{v} - P_I/P\bar{v}}{1 - P_I/P\bar{v}}$$

$$= \left[\left(\frac{\lambda + \dot{V}_A/\dot{Q}\cdot P_I/P\bar{v}}{\lambda + \dot{V}_A/\dot{Q}}\right) - (P_I/P\bar{v})\right] \Big/ [1 - (P_I/P\bar{v})]$$

$$= \frac{\lambda + (\dot{V}_A/\dot{Q})\cdot(P_I/P\dot{v}) - \lambda(P_I/P\bar{v}) - (\dot{V}_A/\dot{Q})\cdot(P_I/P\bar{v})}{(\lambda + \dot{V}_A/\dot{Q})(1 - P_I/P\bar{v})}$$

$$= \frac{\lambda}{\lambda + \dot{V}_A/\dot{Q}} \qquad (4A)$$

where R_c is corrected retention and use of *Eq. A3* with the standard MIGET algorithm would be accurate as a result.

Now, the remaining question is, How much error is caused by use of algorithm (*Eq. A3*) when the proper consideration of inspired krypton requires *Eq. A1*, not *Eq. A2*?

Here

$$3A)_c = \frac{Pa - P_I}{P\bar{v} - P_I}$$

$$= \left\{\left[\frac{\lambda + (\dot{V}_I/\dot{Q})\cdot(P_I/P\bar{v})}{\lambda + \dot{V}_A/\dot{Q}}\right] - (P_I/P\bar{v})\right\} \Big/ [1 - (P_I/P\bar{v})]$$

$$= \frac{\lambda + (\dot{V}_I/\dot{Q})\cdot(P_I/P\bar{v}) - \lambda(P_I/P\bar{v}) - (\dot{V}_A/\dot{Q})(P_I/P\bar{v})}{(\lambda + \dot{V}_A/\dot{Q})[1 - (P_I/P\bar{v})]} \qquad (5A)$$

$$= \frac{\lambda[1 - (P_I/P\bar{v})] + [(\dot{V}_I/\dot{Q}) - (\dot{V}_A/\dot{Q})](P_I/P\bar{v})}{[\lambda + (\dot{V}_A/\dot{Q})][1 - (P_I/P\bar{v})]}$$

$$= \frac{\lambda + [(\dot{V}_I/\dot{Q}) - (\dot{V}_A/\dot{Q})][(P_I/P\bar{v})/[1 - (P_I/P\bar{v})]]}{\lambda + \dot{V}_A/\dot{Q}}$$

We answered this question in three examples of data collected in the present study: *1*) normal lungs, $FI_{O_2} = 0.21$; *2*) injured lungs, $FI_{O_2} = 0.21$; and *3*) injured lungs, $FI_{O_2} = 1.00$. To do this, we calculated Rc from either *Eq. A4* or *Eq. A5*, $\dot{V}_A/\dot{Q}$ compartment by $\dot{V}_A/\dot{Q}$ compartment, with knowledge of $\dot{V}_I/\dot{Q}$ and $\dot{V}_A/\dot{Q}$ for each compartment from the oxygen and carbon dioxide calculation parts of the MIGET program, as well as measured values of $P_I/P\bar{v}$. The results are summarized in Table 6.

As Table 6 shows, prior correction by subtraction of P_I from Pa, $P\bar{E}$, and $P\bar{v}$ produces no error in normal or injured lungs of animals breathing room air. With animals breathing 100% oxygen, there is a minor perturbation of the results (shown in *sheep 171*), but the effects are clinically insignificant and are less than the natural variability in data due to technical errors or minor alterations in physiological state over time.

We are greatly indebted to Dr. David Strom for adjusting the multiple inert gas elimination technique programs to the VAX computer system, Avery A. Johnson for developing and maintaining the gas chromotography-mass spectrometry system, and Dr. Gene B. Hubbard for pathological evaluations. We gratefully acknowledge Dr. Peter Westfall for suggestions concerning the statistical treatment of ventilation-perfusion ratio data. We also acknowledge Rebecca Bexar,

Calvin R. Kennedy, and John Q. Hester for assistance in conducting the experiment.

The opinions or assertions contained herein are the private views of the authors and are not to be construed as official or as reflecting the views of the Department of the Army or the Department of Defense. Citations of commerical organizations and trade names in this report do not constitute an official Department of the Army endorsement or approval of the products or services of these organizations.

Address for reprint requests: Library Branch, US Army Institute of Surgical Research, Ft. Sam Houston, San Antonio, TX 78234-5012.

Received 24 July 1995; accepted in final form 24 June 1996.

REFERENCES

1. **Abdi, S., D. N. Herndon, L. D. Traber, K. D. Ashley, J. C. Stothert, Jr., J. Mauire, R. Butler, and D. L. Traber.** Lung edema formation following inhalation injury: role of the bronchial blood flow. *J. Appl. Physiol.* 71: 727–734, 1991.
2. **Booth, N. H.** Hypnotics and analgesics. In: *Veterinary Pharmacology and Therapeutics*, edited by L. M. Jones. Ames: Iowa State Univ. Press, 1965, p. 182–207.
3. **Comroe, J. H.** *Physiology of Respiration*. Chicago, IL: Year Book Medical, 1974, p. 124.
4. **Dantzker, D. R., P. D. Wagner, and J. B. West.** Instability of lung units with low $\dot{V}_A/\dot{Q}$ ratios during O_2 breathing. *J. Appl. Physiol.* 38: 886–895, 1975.
5. **Derks, C. M., A. A. D'Hollander, and D. Jacobovitz-Derks.** Gas exchange and respiratory mechanics in moderate and severe pulmonary oedema in dogs. *Bull. Eur. Physiopathol. Respir.* 17: 163–177, 1981.
6. **Dixon, W. J.** (Editor). *BMDP Statistical Software*. Berkeley: Univ. of California Press, 1985, p. 105–115.
7. **Dougherty, R. W., M. J. Allison, and C. H. Mullenax.** Physiological disposition of C^{14}-labeled rumen gases in sheep and goats. *Am. J. Physiol.* 207: 1181–1188, 1964.
8. **Dressler, D. P., W. A. Skornik, and S. Kupersmith.** Corticosteroid treatment of experimental smoke inhalation. *Ann. Surg.* 183: 46–52, 1976.
9. **Gale, G. E., J. R. Torre-Bueno, R. E. Moon, H. A. Saltzman, and P. D. Wagner.** Ventilation-perfusion inequality in normal humans during exercise at sea level and simulated altitude. *J. Appl. Physiol.* 58: 978–988, 1985.
10. **Hlastala, M. P., H. T. Robertson, and B. K. Ross.** Gas exchange abnormalities produced by venous gas emboli. *Respir. Physiol.* 36: 1–17, 1979.
11. **Horovitz, J. H.** Selected reports from the proceedings of the second conference on supportive therapy in burn care. Smoke inhalation. *J. Burn Care Rehab.* 2: 265, 1981.
12. **Hubbard, G. B., P. C. Langlinais, T. Shimazu, C. V. Okerberg, A. D. Mason, Jr., and B. A. Pruitt, Jr.** The morphology of smoke inhalation injury in sheep. *J. Trauma* 31: 1477–1486, 1991.
13. **Nunn, J. F.** Anesthesia and the lung. *Anesthesiology* 52: 107–108, 1980.
14. **Powell, F. L., F. A. Lopez, and P. D. Wagner.** Effects of acetone in heparin on the multiple inert gas elimination technique. *J. Appl. Physiol.* 58: 1143–1147, 1985.
15. **Powell, F. L., and P. D. Wagner.** Measurement of continuous distributions of ventilation-perfusion in non-alveolar lungs. *Respir. Physiol.* 48: 219–232, 1982.
16. **Robinson, N. B., L. D. Hudson, H. T. Robertson, D. R. Thorning, C. J. Carrico, and D. M. Heimbach.** Ventilation and perfusion alterations after smoke inhalation injury. *Surgery St. Louis* 90: 352–363, 1981.
17. **SAS Institute.** *SAS User's Guide: Statistics, Version 5*. Cary, NC: SAS Institute, 1985, p. 433–506.
18. **Schoene, R. B., H. T. Robertson, D. R. Thorning, S. C. Springmeyer, M. P. Hlastala, and F. W. Cheney.** Pathophysiological patterns of resolution from acute oleic acid lung injury in the dog. *J. Appl. Physiol.* 56: 472–481, 1984.
19. **Shimazu, T, H. Ikeuchi, A. A. Johnson, G. B. Hubbard, A. D. Maosn, Jr., and B. A. Pruitt, Jr.** Effects of PEEP on ventilation-perfusion ratios following smoke inhalation injury in a sheep model (Abstract). *Proc. Am. Burn Assoc.* 19: 155, 1987.
20. **Shimazu, T., T. Yukioka, G. B. Hubbard, P. C. Langlinais, A. D. Mason, Jr., and B. A. Pruitt, Jr.** A dose-responsive model of smoke inhalation injury: severity-related alteration in cardiopulmonary function. *Ann. Surg.* 206: 89–98, 1987.
21. **Shirani, K. Z., B. A. Pruitt, Jr., and A. D. Mason, Jr.** The influence of inhalation injury and pneumonia on burn mortality. *Ann. Surg.* 205: 82–87, 1987.
22. **Stollery, D. E., R. L. Jones, and E. G. King.** Dead space ventilation: a significant factor in respiratory failure after thermal inhalation. *Crit. Care Med.* 15: 260–261, 1987.
23. **Wagner, P. D., G. Hedenstierna, G. Bylin, and L. Lagerstrand.** Reproducibility of the multiple inert gas elimination technique. *J. Appl. Physiol.* 62: 1740–1746, 1987.
24. **Wagner, P. D., R. B. Laravuso, E. Goldzimmer, P. F. Naumann, and J. B. West.** Distribution of ventilation-perfusion ratios in dog with normal and abnormal lungs. *J. Appl. Physiol.* 38: 1099–1109, 1975.
25. **Wagner, P. D., and F. A. Lopez.** Gas chromatography techniques in respiratory physiology. In: *Techniques in the Life Sciences*, edited by A. B. Otis. County Clare, Ireland: Elsevier, 1984, p. 403/1–403/24.
26. **Wagner, P. D., P. F. Naumann, and R. B. Laravuso.** Simultaneous measurement of eight foreign gases in blood by gas chromatography. *J. Appl. Physiol.* 36: 600–605, 1974.
27. **Wagner, P. D., and R. Rodriguez-Roisin.** Clinical advances in pulmonary gas exchange. *Am. Rev. Respir. Dis.* 143: 883–888, 1991.
28. **Wagner, P. D., H. A. Saltzman, and J. B. West.** Measurement of continuous distribution of ventilation-perfusion ratios: theory. *J. Appl. Physiol.* 36: 588–599, 1974.